Engineering and Technology Journal
Journal homepage: https://etj.uotechnology.edu.iq

Computational Single and Multiphase Approaches to Investigate the Hydrothermal Behavior of Hybrid Nano-fluid in Plain and Wavy Tubes

Ahmed S. Habeeb[a,b*], **Sattar Aljabair**[a], **Abdulhassan A. Karamallah**[a]

[a] Mechanical Engineering Department, University of Technology, Alsina'a Street, 10066 Baghdad, Iraq.
[b]A Biomedical Engineering, College of Engineering, University of Warith Al-Anbiyaa, Karbala.
*Corresponding author Email: ahmedsabahalhilali@gmail.com

HIGHLIGHTS

- A new type of hybrid Nano-fluid (Fe_3O_4 – MgO/H_2O) was used.
- Plain and wavy tubes with turbulent flow were considered.
- Two-phase models were employed for the numerical simulation.
- The HTC enhancement appears to be more pronounced at φ = 2% in both tubes.
- HTC increment is slightly higher with a wavy-walled tube than the plain one.

ARTICLE INFO

Handling editor: Muhsin Jweeg

Keywords:
Heat transfer; Multiphase Approach; Wavy wall tube; Hybrid Nano-fluids; Fe_3O_4+MgO.

ABSTRACT

The newest class of heat transfer improvement is accomplished by using hybrid Nano-fluids. Therefore, the heat transfer and pressure drop of a mixture of Iron oxide (Fe_3O_4) and Magnesium oxide (MgO) nanoparticles suspended into the base fluid under a turbulent regime through a plain and wavy tube are computed employing commercial software ANSYS Fluent. A mixture of Fe_3O_4 and MgO nanoparticles in pure water is considered a brand-new type of hybrid Nano-fluid for boosting heat transfer. The simulation procedures were performed utilizing the single and multiphase (mixture) approaches at Reynolds number in the range of (3,916 - 31,331) and volume concentrations range of ($0.5\% \leq \varphi \leq 2\%$). The plain and wavy walls are subjected to a constant heat flux of 18,189 W/m^2, and the flow is presumed as fully developed. The computed outcomes are validated with the correlation equations and experimental data of literature. The outcomes demonstrate that boosting the nanoadditives fraction leads to a remarkable improvement of heat transfer and hydrothermal performance indicator (HPI) of MgO-Fe_3O_4 /H_2O Hybrid Nano-fluid through the considered tubes compared with the conventional base fluid. However, the increment is slightly higher with a wavy wall tube than with the plain one. Moreover, new correlations were suggested for specific water-based hybrid Nano-fluid volume concentrations.

1. Introduction

Nano-fluids have obtained a significant concentration in many applications such as microelectronics, refrigeration, transportation, nuclear, and solar technologies. They have gained considerable attention due to their ultrahigh thermal efficiency. The nanoparticles enhance the suspension stability, and the flexible thermophysical properties, and extend the interface of a solid particle due to their efficient surface area at low concentrations [1, 2]. However, the channel clogging and sedimentation cause pressure through the flow. The hydrothermal characteristics of the Nano-fluids are based on morphology, temperature, nanoparticles loading, and the thermophysical properties of the base fluids [3, 4].

For expensive empirical investigations, the evaluation of hydrothermal properties of Nano-fluids significantly relies on their proper modeling. The appropriate simulation of Nano-fluids demands an excellent knowledge of the physical phenomena which causes augmentation in the thermal conductivity [5,6]. There are several mechanisms responsible for developing thermal conductivity. These mechanisms are Brownian motion, thermophoresis, lift and drag forces, the interface layering of the liquid molecules around the nanoadditives, and clustering and diffusion of nanoparticles [7-9].

Homogeneous and multiphase approaches are the most common computational techniques utilized in simulating the HTC and characteristics of Nano-fluids flow. In a homogeneous model, the Nano-fluids are presumed to be a homogenous mixture, i.e., nanoparticles and fluid move without slip and with equal temperature and velocity [10-12]. Meanwhile, the CFD multiphase approaches are classified into Lagrangian-Eulerian and Eulerian–Eulerian according to the treatment of fluid and nanoparticle phases. This model consists of three numerical models: mixture, Eulerian, and volume of fluid (VOF) models. The mixture model

http://doi.org/10.30684/etj.2023.136449.1316
Received 20 October 2022; Accepted 14 January 2023; Available online 31 January 2023

is the most straightforward multiphase numerical approach as it performs for various particle sizes, exceptionally tiny particles. The nanoparticles follow the flow with a potent combination of fluid and particle phases[13].

Nevertheless, selecting the accurate approach among single and multiphase numerical models is still debatable. Numerous researchers affirmed the accuracy of the homogenous model, which is a widely used approach, simple, and cost-efficient [9, 14-18]. Despite this, few researchers approved the opposite due to neglecting the significant effect of interactive interphase forces [19-26]. Labib et al. [27] computed the HTC of Al_2O_3/CNTs/H_2O and a combination of Al_2O_3/EG/H_2O hybrid Nano-fluids flow using a mixture model. The hybrid Nano-fluids flow inside a plain tube under a laminar regime with wall-fixed heat flux. The researchers found that hybrid Nano-fluids gave a more noticeable HTC (59.86)% than mono Nano-fluids. Also, they found that the increment in heat transfer was less pronounced when water was utilized as base fluid than EG. Kumar and Puranik [28] investigated the flow aspects of three types of Nano-fluids, including TiO_2/water, Cu/water, and Al_2O_3/water. They revealed that the homogenous approach is more precise than the Lagrangian-Eulerian approach at a volume fraction greater or equal to (0.5) % and less or equal to (2)%. Hejazian et al. [29] employed the mixture and Eulerian models to study the thermal and hydrodynamics properties of water-based Al_2O_3 Nano-fluid at volume fractions ($0.1\% \leq \varphi \leq 2\%$). The researchers showed that the findings predicted by both approaches were very akin to the empirical outcomes.

On the contrary, Göktepe et al. [30] demonstrated that the mixture approach was less precise than homogenous and Eulerian models. The authors simulated the hydrothermal characteristics of water-based Nano-fluid with concentrations ($0.6\% \leq \varphi \leq 1.6\%$). Davarnejad and Jamshidzadeh [31] explored the turbulent heat transfer behavior of MgO/H_2O Nano-fluid flow through a flat tube employing homogenous, VOF, and mixture models. The researchers reported that the simulated results agreed with the empirical data. They revealed that augmentation of the nanoadditives concentrations increases the Nusselt number (Nu) and pressure drop losses. However, the increment of pressure drop was minor compared with the Nu. They also concluded that the mixture and VOF models were more precise than the homogenous model for predicting heat transfer at high nanoparticle concentration. The average deviations from the empirical data were around 2% and 11% for multiphase and single-phase models, respectively. However, Lotfi et al. [32] and Behroyan et al. [18] underpredicted the HTC computed using the Eulerian approach for water-based Al_2O_3 at (2-7) % and water-based Cu Nano-fluid at (1- 2)%, respectively. Nevertheless, Ebrahimnia-Bajestan et al. [26] overpredicted the HTC of water-based TiO2 at (1- 2.3)%. Akbari et al.[33, 34] overestimated the computed HTC of water-based Al_2O_3 Nano-fluid at concentrations (0.6 - 1.6) vol. % employing the mixture, VOF, and Eulerian approaches.

Moreover, Sundar et al. [35] computed the HTC of (Fe_3O_4-MWCNT/ H_2O) hybrid Nano-fluid through a flat (circ (tube. The results demonstrated that the HTC increased by 32% at Re (22× 〖10〗 ^3) and (0.3)%. Li et al. [36] studied the impact of Re, concentration, and amplitude on the performance of (MgO/Ag/H_2O) hybrid Nano-fluid along a sinusoidal tube. The outcomes revealed that an increase in the wavy amplitudes resulted in minimizing the performance evaluation criteria.

Furthermore, Rashidi et al. [37] compared the numerical homogenous model with VOF, mixture, and Eulerian approaches of Cu/H_2O Nano-fluid flow along a wavy channel. The findings revealed that the predicted HTC by the homogenous model augmented with increasing the volume concentrations for all Reynolds numbers. In contrast, the computed HTC by multi-phase numerical models enhanced in the middle and front of the wavy channel and decreased at low Reynolds numbers throughout the channel. Alshare et al. [38] studied the thermal and hydrodynamics flow of Al_2O_3–Cu /H_2O hybrid Nano-fluids under steady temperature in a wavy channel for Reynolds numbers (102 –103), and nanoparticle fractions range from (1-2)%. Findings revealed that the friction factor and HTC increased with increasing the nanoparticles' volume fraction. The Nanoparticle's volume concentration of 1% and 2% resulted in a minimal increase in heat transfer. However, adding 1% and 2% volume fraction hybrid nanoparticles increased the Nusselt number by 16% and 22%. Similarly, increasing the channel wavy amplitude boosted the HTC by 12 %, and frictional losses increased to (15)%.

Several review articles concentrated on conducting the numerical single-phase and multiphase modeling of Nano-fluids with all the related physical mechanisms to set the fundamental findings [39-41]. Based on the literature, the experimental and numerical work on hybrid Nano-fluids is limited and few researchers considered the mixture of various types of nanoadditives. Hence, in this paper, the single and multiphase (mixture) numerical approaches are investigated to simulate the hydrothermal characteristics and nanoparticles migration of a new hybrid Nano-fluid consisting of Fe_3O_4-MgO/H_2O through a horizontal plain and wavy tube under turbulent conditions.

2. Problem Description

The hybrid Nano-fluid containing spherical nanoparticles of water-based Fe_3O_4/MgO (50% Fe_3O_4 and 50% MgO) by volume flow through horizontal plain and wavy tubes is considered. The thermophysical characteristics of water, MgO, and Fe_3O_4 nano-additives are given in Table 1. These hybrid nanoparticles are mixed for the first time with water by considering volume concentrations of $0.5\% \leq \varphi \leq 2\%$. The tube wall is subjected to a constant heat flux of 18,189 W/m^2 with Reynolds numbers (3,916 to 31,331), and the flow is assumed as fully developed. The hybrid nanoadditives are presumed to be diffused homogenously into the water without any surfactants. The average diameter of nanoadditives is deemed to be (20) nm. Figure1 illustrates the schematic diagram of the plain and wavy tube with a length (L) of (1000) mm and a hydraulic diameter (Dh) of (14) mm.

Table 1: The characteristics of pure water and nanoadditives [42-44]

Properties	H_2O	MgO	Fe_3O_4
Density (kg m^{-3})	997	3560	5180
Specific heat (J kg^{-1} K^{-1})	4180	955	670
Thermal conductivity (W m^{-1} K^{-1})	0.607	45	80.4
Dynamic viscosity (kg m^{-1} s^{-1})	0.000891	---	---

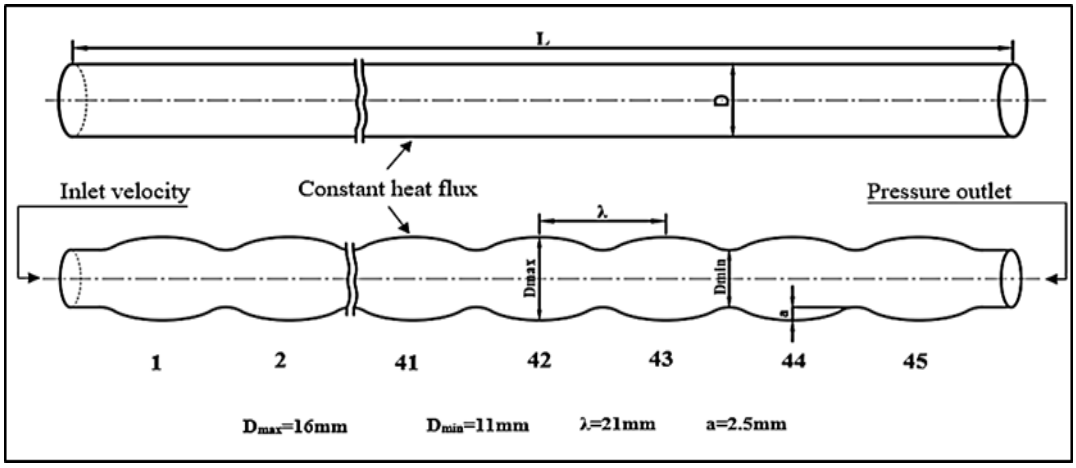

Figure 1: Schematic of plain and wavy tubes

3. Mathematical Formulation

3.1 Single-Phase Model

The accuracy of the single-phase model mainly depends on the accurate estimation of the Nano-fluid thermophysical properties. The mixture is assumed as a homogenous fluid with negligible slip motion between fluid and nanoparticles. The liquid and nanoadditives are also presumed to be hydrodynamically and thermally at equilibrium with each other. The governing equations of this approach are given as follows:

Continuity equation:

$$\nabla.\left(\rho_{nf}\, u_{nf}\right) = 0 \tag{1}$$

Momentum equation:

$$\nabla.\left(\rho_{nf}\, u_{nf}\, u_{nf}\right) = -\nabla p + \nabla.\left(\mu_{nf}\nabla u_{nf}\right) + \rho_{nf}\, g \tag{2}$$

Energy equation:

$$\nabla.\left(\rho_{nf}\ c_{p,nf}\, u_{nf}\, T_{nf}\right) = \nabla.(k_{nf}\, \nabla T_{nf} \tag{3}$$

3.2 Numerical Multiphase Mixture Approach

The mixture model is designed for more than two phases and the relative velocity among phases is determined using correlation. The primary phase (fluid) impacts the secondary phase (particulate) through turbulence and drag forces; the particulate phase influences the fluid phase by minimizing its mean momentum. This approach computes (the continuity, energy, momentum) of the mixture, and the concentrations for the secondary phases [41].

The governing equations of the mixture approach can be expressed as:

Continuity Equation:

$$\nabla.(\rho_{nf}\, u_{nf}) = 0 \tag{4}$$

Momentum equation:

$$\nabla.\left(\rho_{nf}\, u_{nf}\, u_{nf}\right) = -\nabla P + \nabla.\left(\mu_{nf}\nabla u_{nf}\right) + \nabla.\left(\varphi_f\, \rho_f u_{dr,f} + \varphi_{np}\, \rho_{np} u_{dr,np} u_{dr,np}\right) + \rho_{nf}\, g \tag{5}$$

Energy equation:

$$\nabla.\left(\varphi_f u_{nf}\rho_f\ C_{P,f}T_f + \varphi_{np}u_{np}\,\rho_{np}\ C_{P,np}T_{np}\ \right) = \nabla.\left[\left(\varphi_f\ \mathrm{k}_f + \varphi_{np}\ \mathrm{k}_{np}\right)\nabla \mathrm{T}\right] \quad (6)$$

Volume fraction:

$$\sum_{i=1}^{n}\varphi_i = 1 \quad (1)$$

$$\nabla.\left(\varphi_{np}\ \rho_{np}u_{nf}\right) = -\nabla.\left(\varphi_{np}\rho_{np}u_{dr,np}\right) \quad (8)$$

Characteristics equations of hybrid Nano-fluids are expressed as:
Density:

$$\rho_{nf} = \varphi_f\ \rho_f + \sum \varphi_{np}\ \rho_{np} \quad (9)$$

Viscosity:

$$\mu_{nf} = \varphi_f\ \mu_f + \sum \varphi_{np}\mu_{np} \quad (10)$$

Mixture velocity:

$$\mathrm{u}_{nf} = \frac{\varphi_f\rho_f\ \mathrm{u}_f + \sum \varphi_{np}\rho_{np}\mathrm{u}_{np}}{\rho_{nf}} \quad (11)$$

Thermal conductivity:

$$k_{nf} = \varphi_f\ k_f + \sum \varphi_{np}\ k_{np} \quad (12)$$

The drift velocity of base fluid:

$$\mathrm{u}_{dr,f} = \mathrm{u}_f - u_{nf} \quad (13)$$

The drift velocity for nanoadditives phase:

$$\mathrm{u}_{dr,np} = \mathrm{u}_{np} - u_{nf} \quad (14)$$

Abbasi and Baniamerian [45] and Hatami et al. [46] suggested the relative velocity and the drag force, respectively, as given below:

$$u_{f,np} = \frac{\rho_{np}\ d_{np}^2}{18\ \mu_f\ f_D}\ \frac{(\ \rho_f - \rho_{nf}\ )}{\rho_f}\ \ \left(g - \left(u_{nf}.\nabla\right)u_{nf}\right) \quad (15)$$

Drag force is expressed as:

$$f_D = \begin{cases} 1 + 0.15\ Re_{np}^{0.687} & Re_{np} \le 1000 \\ 0.0183 Re_{np} & Re_{np} > 1000 \end{cases} \quad (16)$$

Where:

$$Re_{np} = \frac{u_{nf}\ d_{np}\ \rho_{nf}}{\mu_{nf}} \quad (17)$$

Where: d_{np} denotes the diameter of nanoadditives.
Launder and Spalding's (k-ε) model was expressed in Eqs. (18) and (19).

$$\nabla.(\ \rho_m\ \ \mathrm{v}_k) = \nabla.(\ \frac{\mu_{t,m}}{\sigma_k}\ \nabla \mathrm{k}) + \ \ \mathrm{G}_m - \ \rho_m\,\varepsilon \quad (18)$$

$$\nabla.(\ \rho_m\ \ \mathrm{v}_\varepsilon) = \nabla.(\ \frac{\mu_{t,m}}{\sigma_\varepsilon}\ \nabla \varepsilon) + \frac{\varepsilon}{k}\ (\ C_1\ \mathrm{G}_m - C_1\ \rho_m\ \varepsilon) \quad (19)$$

Where:

$\mu_{t,m} = \rho_m\ C_\mu\ \frac{k^2}{\varepsilon}$, and the constants are $C_1 = 1.44, C_2 = 1.92, \sigma_\varepsilon = 1.3$ and $\sigma_k = 1.0$

4. Numerical Description and Grid Independency

This paper performs the numerical simulation using the finite volume method-based commercial software ANSYS Fluent (version: 19.3). The semi-implicit pressure-linked equations (SIMPLE) technique was used for pressure-velocity coupling. The first-order upwind scheme is applied to discretize volume fraction in the mixture approach. Meanwhile, the second-order upwind technique discretizes the convective terms. Grid independence tests are implemented to check the accuracy of the findings. The mesh is finer near the tube wall to capture the boundary layer (thermal-viscous) and the temperature gradient. The boundary conditions are modeled by employing a 3D computational domain, as depicted in Figure 2 (a,b, and c). The boundary conditions of constant heat flux, velocity inlet, and pressure outlet are respectively defined at the wall, tube's inlet, and outlet as depicted in Figure 1 . For the convergence criteria, the residuals of all parameters are set to less than 10^{-6}.

A structured hexahedral grid is generated and applied along the tested section, as shown in Figure2 (a,b, and c). Five mesh sizes were tested and presented in Table 2. The values of ΔP and $Nu_{av.}$ for pure water at Re (7832) were found approximately constant using grids 3, 4, and 5, with the highest deviation less than 0.1%, as depicted in Figure 3(a and b). Hence, grid 3 is applied for all the computations to guarantee the accuracy is kept at less running time and computational cost.

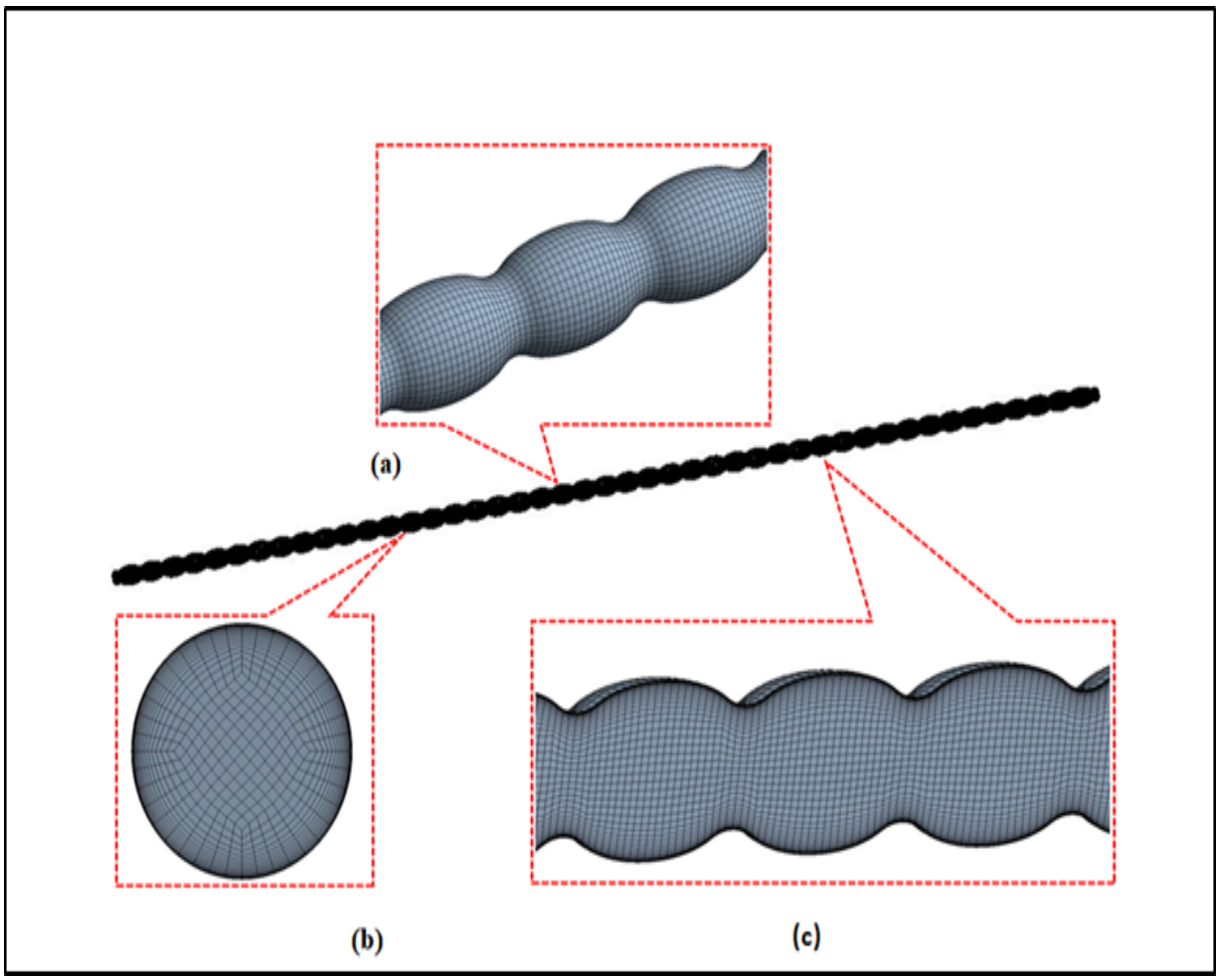

Figure 2: Mesh configuration (a) surface, (b) section, and (c) interior.

Table 2: The analysis of mesh sizes on Nuav and ΔP

Grid type	Elements	Average Nusselt number	Pressure drop (pa)
Coarse (1)	458605	51.64	285.88
Medium (2)	1052573	51.61	282.01
Fine (3)	1001000	51.59	279.99
Very Fine (4) (5)	1344408	51.59	279.76
	1645000	51.59	279.70

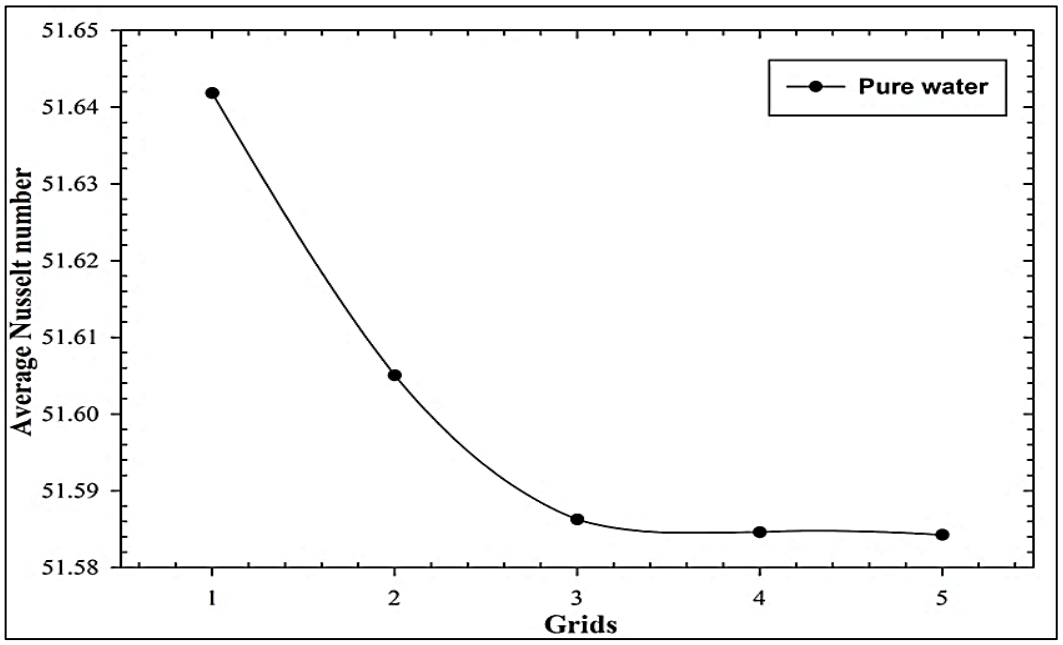

(a)

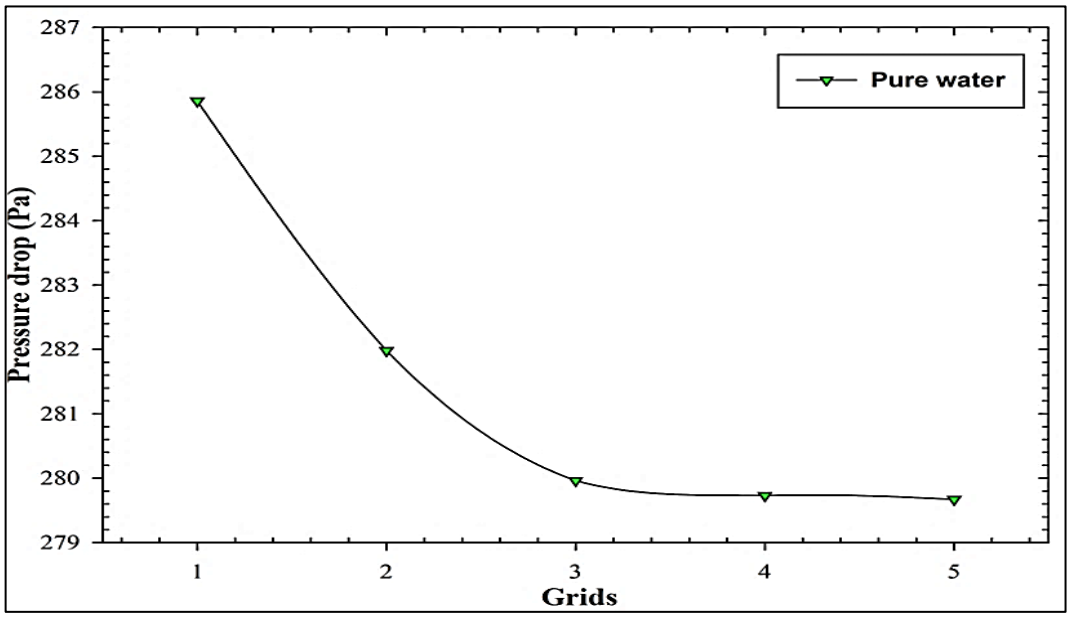

(b)

Figure 3: Analysis of grid sensitivity (a) average Nusselt number, and (b) pressure drop

5. Results and Discussion

This section investigated the HTC, friction factor, and hydrothermal performance indicator of water based Fe_3O_4 / MgO hybrid Nano-fluid in plain and wavy tubes employing the mixture approach. The volume concentrations of the nanoadditives range from ($0.5\% \leq \varphi \leq 2\%$), and the Reynolds number ranges from 3,916 to 31,331. The computed results of the plain and wavy tube will be assessed and compared with the relevant studies.

5.1 Validation

Several numerical calculations were performed on pure water to validate the reliability of the numerical findings and provide a baseline for comparison of the Nano-fluids data. Thus, The outcomes of the Nusselt number were compared with the empirical data of Maddah et al. [47], Notter and Sleicher [48], and Dittus–Boelter [49] correlations for the turbulent flow.

1) Notter and Sleicher equation [48]:

$$\mathrm{Nu} = 5 + 0.015\,\mathrm{Re}^{a}\,Pr^{b} \tag{20}$$

where

$$a = 0.88 - \frac{0.24}{4 + Pr}$$

$$b = 0.33 + 0.5\, e^{(-0.6Pr)}$$

For the range of $0.1 < Pr < 10^4$, $10^4 < Re < 10^6$, and the deviation is $\mp$ 10%.

2) Dittus–Boelter equation [49] is expressed as:

$$Nu = 0.023\, Re^{0.8} Pr^n \tag{21}$$

Where, $n = 0.4$ and 0.3 for heating ($T_s > T_m$) and cooling($T_s < T_m$), respectively.

Figure 4 (a) validates the computed Nusselt number and values obtained from the abovementioned equations for various Reynolds numbers. It is obvious that the Nusselt number values for pure water are very akin to the predictions of Maddah et al. [47], Notter and Sleicher [48], and Dittus–Boelter [49] with an average variation (6.90)%.

The accuracy of the computed friction factor inside the plain tube is evaluated and compared with the experimental results of Maddah et al.[47], Blasius [50], Fang et al. [51], and Petukov [52] for water under turbulent regime.

3) Blasius [50] equation for the turbulent region

For $Re \leq 2 \times 10^4$

$$f = 0.316\, Re^{-0.25} \tag{22}$$

For $Re \geq 2 \times 10^4$

$$f = 0.184\, Re^{-0.2} \tag{23}$$

4) Petukov [52] equation for the turbulent region

$$f = (0.79\, ln(Re) - 1.64)^{-2} \tag{24}$$

For $3000 < Re < 5 \times 10^6$.

5) Fang et al.[51] equation for the turbulent region

$$f = 0.25 \left[log\, \left(\frac{150.39}{Re^{0.98865}} - \frac{152.66}{Re} \right) \right]^{-2} \tag{25}$$

For $3000 \leq Re \leq 10^8$.

The friction factor of the water versus the Reynolds numbers is displayed in Figure 4 (b). This demonstrates that the predicted friction factor agrees with the above-mentioned studies with an average variation of (1.80) %.

5.2 Thermal and Hydrodynamic Characteristics

Figure 5 (a) and (b) depict the findings of the turbulent convective HTC of (0.5, 1, and 2) vol.% the hybrid Nano-fluid employing multiphase (mixture) model along the plain and wavy wall tubes. It can be seen that HTC overpredicts at φ = 2% in both tube types. However, the estimated average HTC was higher for wavy wall tube than the plain tube. It was observed that the average enhancement in HTC obtained from 2% Fe_3O_4-MgO/H_2O hybrid Nano-fluid is (151.6)% through the wavy tube and (113.6)% along the plain tube. This trend is similar to the findings of other researchers [42,53,54]. The hybrid Nano-fluid boosted the heat transfer more significantly than the pure water due to the potent interactivity among the nanoadditives. Also, the crucial reasons of the enhancement in HTC could be due to the significant increment of the thermal conductivity of hybrid Nano-fluid than the conventional fluid. Further, the heat transfer boosted with augmented the ratio of nanoadditives concentrations. The acceleration of the energy exchange process is another mechanism that affects the HTC enhancement due to the chaotic motion of hybrid nanoadditives. The irregular motion can flatten the temperature distribution and lead to a sharp temperature gradient between the wall and hybrid Nano-fluids. Thus, the HTC between the hybrid Nano-fluids and wall would be enhanced [55].

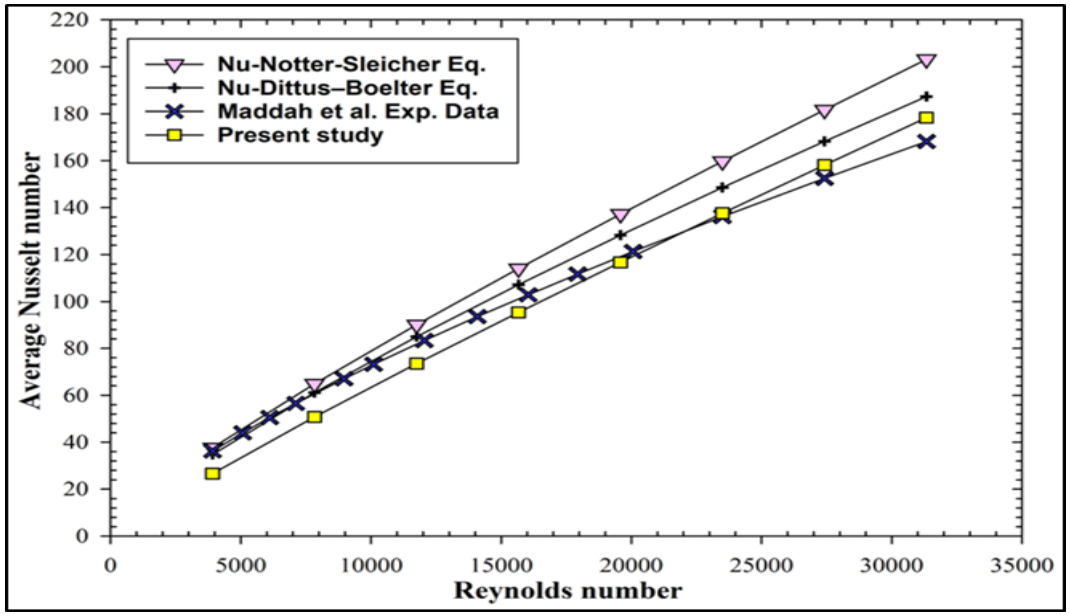

(a)

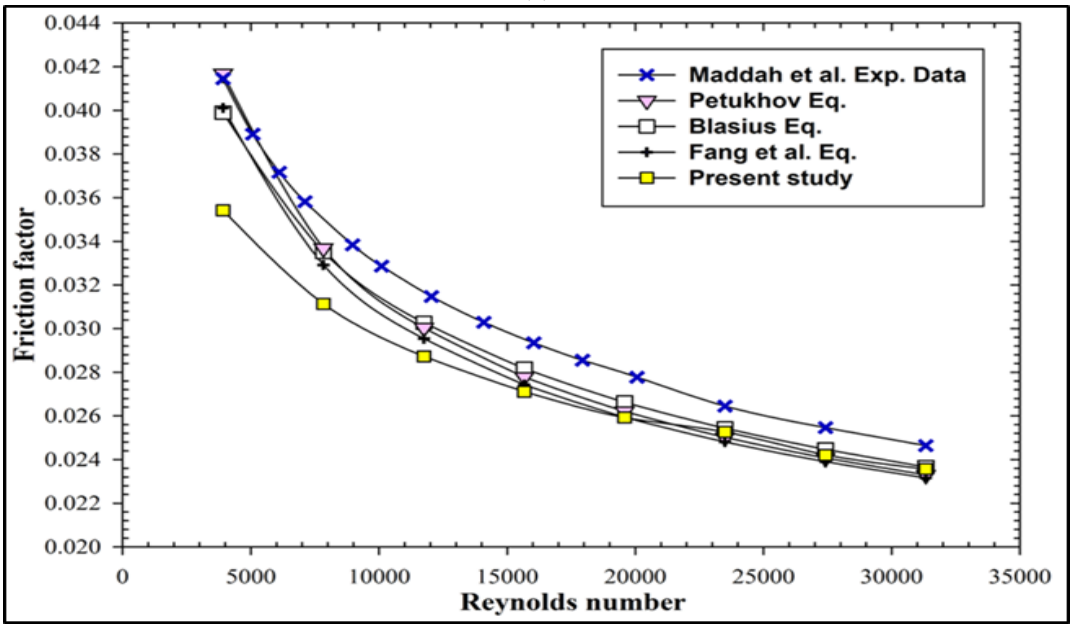

(b)

Figure 4: Validation of the (a) average Nusselt number, and (b) friction factor

A further fundamental parameter of HTC improvement is the generation of secondary flow in the diverging areas, as clearly shown in Figure 7 (a,b, and c). The swirl flow improves the mixing of the hot fluid near the wall with cold fluid in the tube's central region and thus enhances the heat transfer. Also, these recirculation regions explain the advantages of the wavy geometry over the conventional tube in improving the HTC. Figure 7 (a,b, and c) depicts the turbulence intensity, which is boosted in the diverging zones due to eddy formation. Additionally, the random micromotion of nanoparticles enhances the momentum exchange and, consequently, boosts the turbulence intensity, further enhancing the heat transfer. The irregular micromotion develops with raising the volume concentrations of nanoadditives. This agrees with the most recent literature [3,56,57] .

Figure 6 (a) and (b) display the predicted friction factor outcomes inside the plain and wavy tubes at different Reynolds numbers. It can be noticed that the estimated friction factor increases with rising volume concentrations and is disproportional with the Reynolds numbers through both used tubes. Also, the Fe_3O_4-MgO/H_2O hybrid Nano-fluid generates a higher friction factor than base fluid, yet the estimated outcomes are within the acceptable limit. This trend occurs because of the small velocity boundary layer thickness and a slight increase in the viscosity ratio [53]. Additionally, at low Reynolds numbers, the maximum increment of friction factor values was (4.6, 6.6, and 10.2)% in the plain tube, and (43.8, 49.2, and 56.5)% in the wavy tube at volume concentrations (0.5, 1, and 2)%. It was seen that the wavy tube's friction factor is considerably greater compared with the traditional tube due to the role of amplitudes, which increases the pressure drop; this leads to increasing the pumping power consumption.

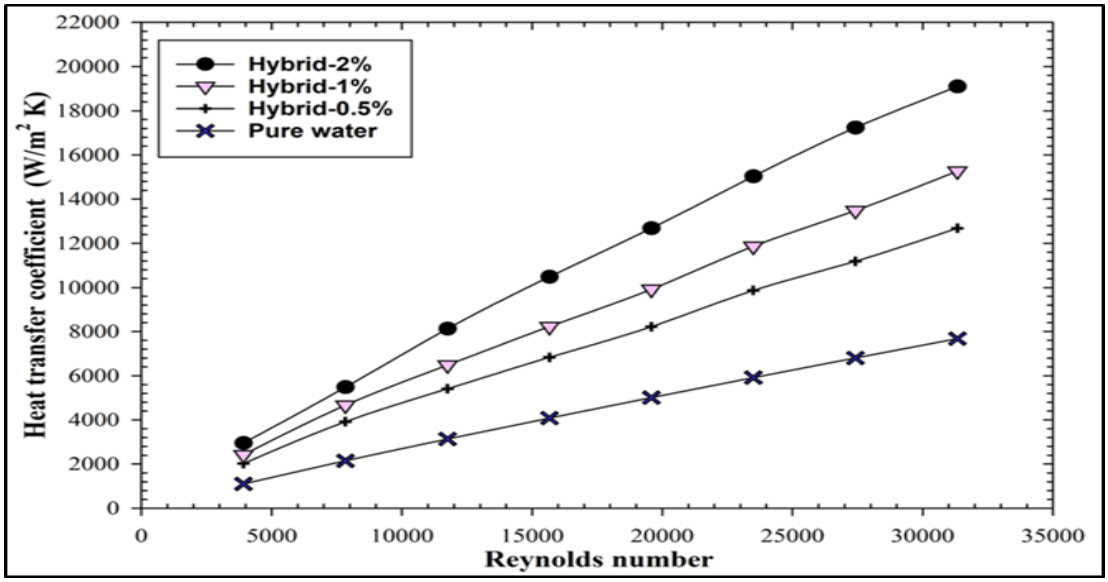

(a)

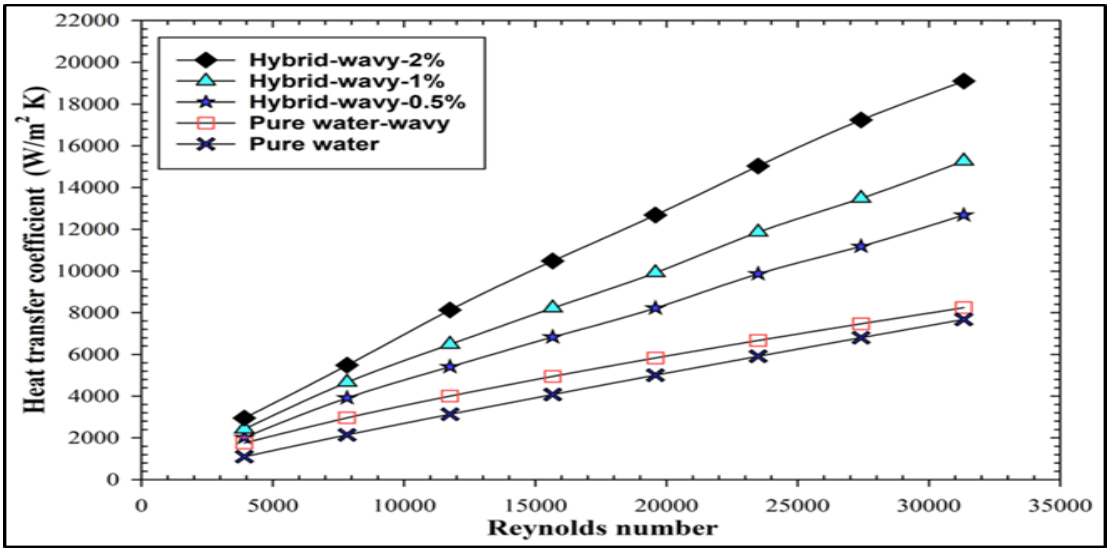

(b)

Figure 5: Heat transfer coefficient of hybrid Nano-fluid and water at various concentrations versus Reynolds number inside (a) plain tube, and (b) wavy tube

5.3 Hydrothermal Performance Indicator (HPI)

The designers always look forward to improving any system's hydraulic and thermal properties, improving the HTC, and reducing pressure losses. The proportion of the heat transfer for the Nano-fluid to the conventional fluid at an identical power consumption is known as the hydrothermal performance indicator (HPI) and can be expressed by:

$$HPI = \left(\frac{\overline{Nu}_{nf}}{\overline{Nu}_{f}}\right).\left(\frac{f_{nf}}{f_{f}}\right)^{-1/3} \tag{26}$$

The impact of hybrid Nano-fluid on the HPI at different volume fractions is illustrated in Figure 8 (a) at low Reynolds number (3916) and Figure 8 (b) at high Reynolds number (31331). The outcomes reveal that HPI of the hybrid Nano-fluid augments with increasing the nanoparticles volume fractions at low and high Reynolds number in both tested tubes. Nevertheless, the computed HPI in the wavy wall tube was fairly greater compared with the plain tube at (Re=3916 and 31331). From Figure 8 (a), the HPI was recorded as (1.6, 1.81, and1.91) and (1.48, 1.63, 1.93, and 2.35) for the nanoadditives fraction of (0, 0.5, 1, and 2)% in the plain and wavy wall tubes, respectively. Meanwhile, the HPI was reported as (1.53, 1.87, and 2.27) in the plain tube and (1.09, 1.59, 1.92, and 2.41) in the wavy tube, at similar volume concentrations, as displayed in Figure 8 (b). Based on the findings, the highest achievable HPI of Fe_3O_4-MgO/H_2O flowing through a wavy wall tube is (2.41) which belongs to the 2% volume fraction at Re=31331. Thus, the nanoadditives volume concentration of 2% is the desirable choice for the designers in providing the best favorable improvement in heat transfer.

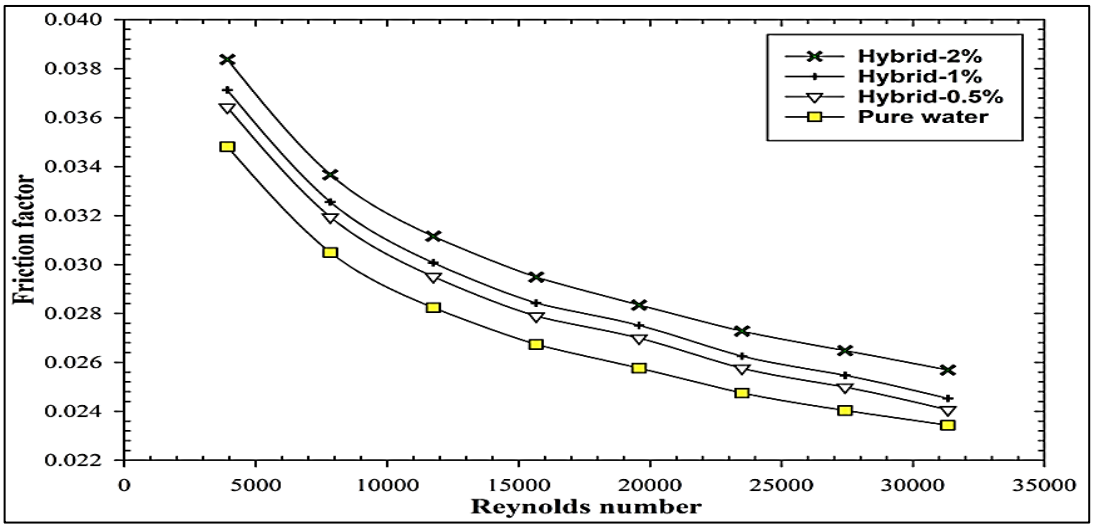

(a)

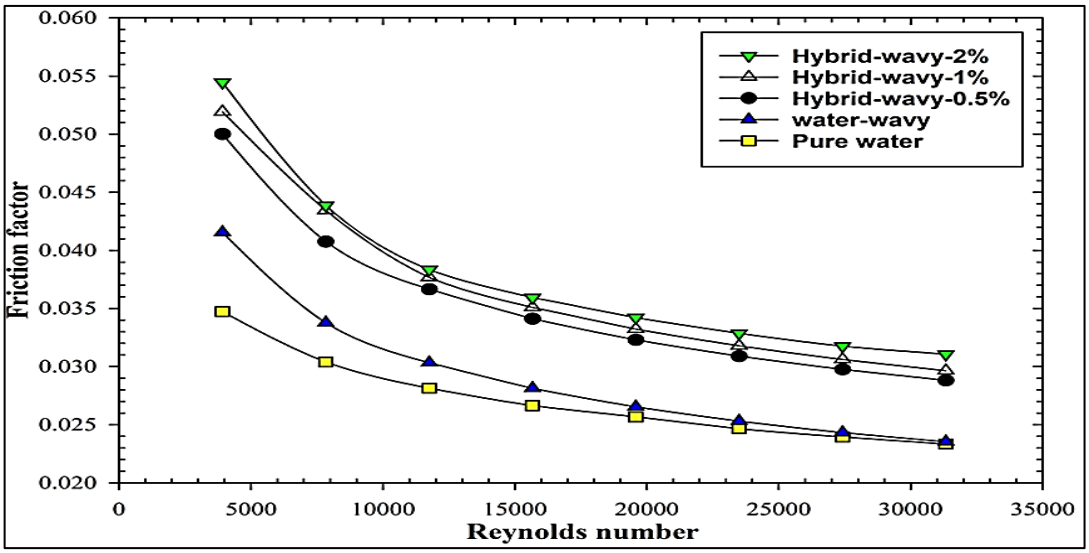

(b)

Figure 6: Friction factor of hybrid Nano-fluid and water at various fractions versus Reynolds number along (a) plain tube, and (b) wavy tube

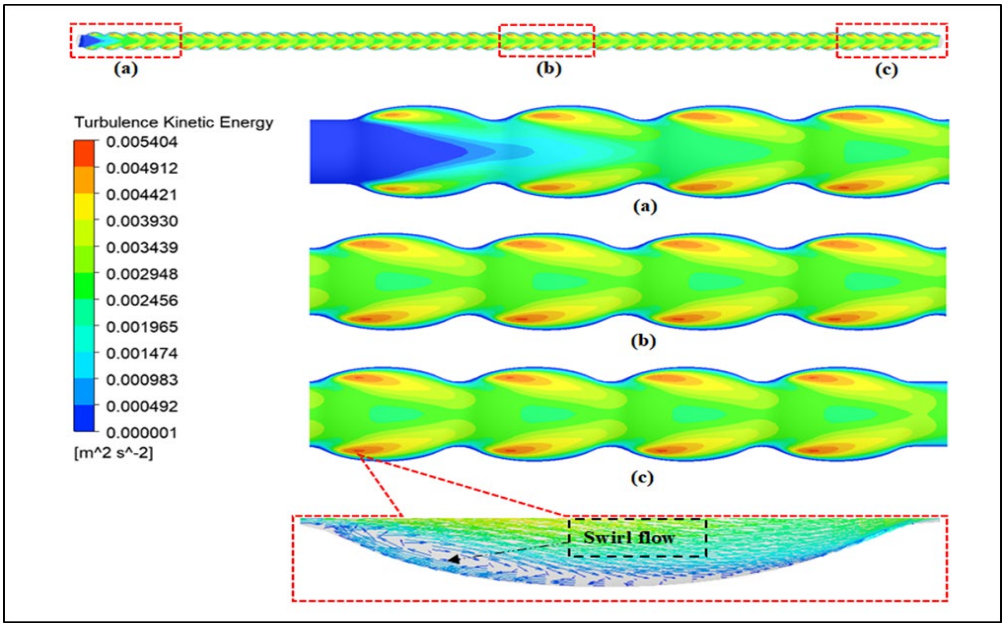

Figure 7: Contours of turbulence intensity at concentration (2%) and Re = 3,916

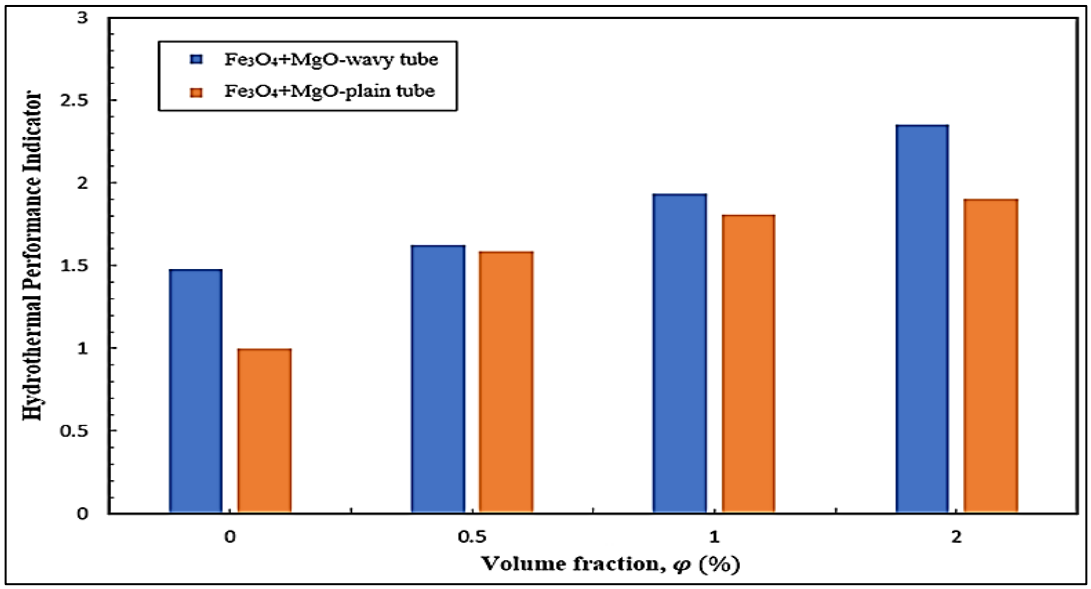

(a)

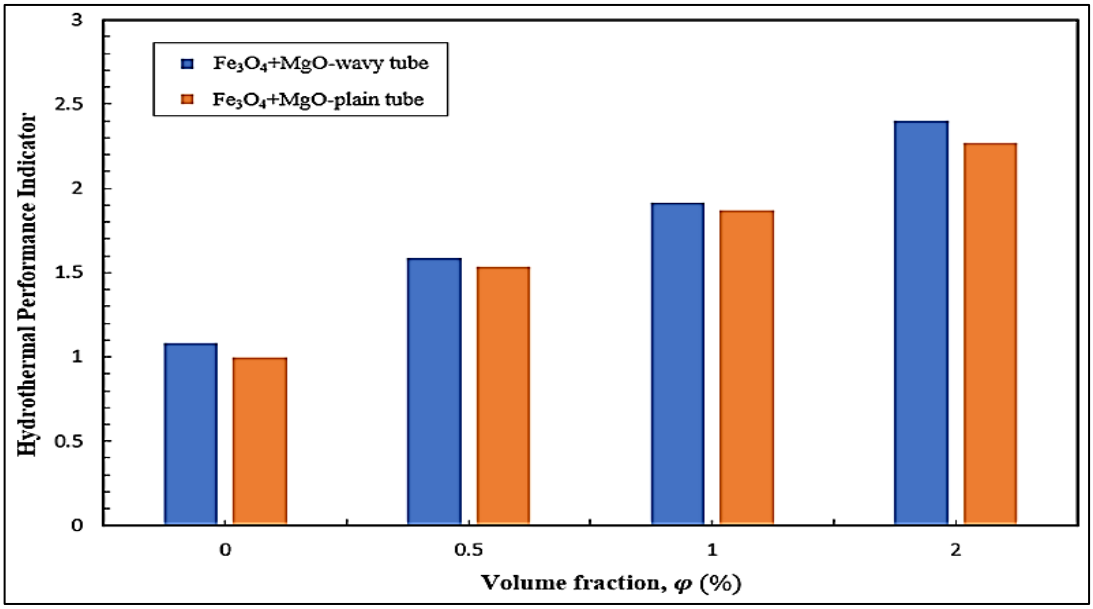

(b)

Figure 8: Hydrothermal performance indicator of hybrid Nano-fluid inside the plain and wavy wall tubes with different volume fractions at (a) Re = 3916; (b) Re = 31331

5.4 Nanoparticles Volume Fraction Contours

The main merit of the multiphase (Mixture) approach is the prediction of the volume concentration distribution. Figure 9 (a-f) depicts the volume fraction distribution contours of 2% Fe_3O_4 + MgO /H_2O hybrid Nano-fluid at Reynolds number of (31,331), along various cross-sections (a to f) of the wavy wall tube. Phase 2 and phase 3 represents Fe_3O_4 and MgO nanoadditives, respectively. The migration of nanoadditives is almost identical at low and high Reynolds numbers along the different cross-sections. This could be attributed to the similar diameter of MgO and Fe_3O_4 nanoparticles. Thus, the distribution of nanoparticles is not influenced by the sorts of nanoadditives. Such findings are in good agreement with [34,58]. Also, the lower Reynolds numbers provide a more uniform distribution of the nanoadditives with the base fluid than higher ones along the tube. Increasing the Reynolds number to (31,331) led to the possibility of clustering and distribution of nanoparticles in the tube center, as depicted in Figure 9 (a-f). At the highest Reynolds number, the diverging and converging zones promote the migration of nanoadditives to the wall due to the generation of eddies in the diverging areas, which led to increase the turbulence energy, as shown in Figure 7 (a,b, and c). Consequently, boosting the heat transfer by reducing the surface temperature of the wall. The thermophoresis forces and Brownian motion could justify the nonuniformity in nanoparticle distribution. These forces may disturb the cross-sectional distribution of nanoparticle volume concentration. Thermophoresis happens intensely close to the wall, whereas the Brownian motion occurs everywhere in the cross-section [59,60].

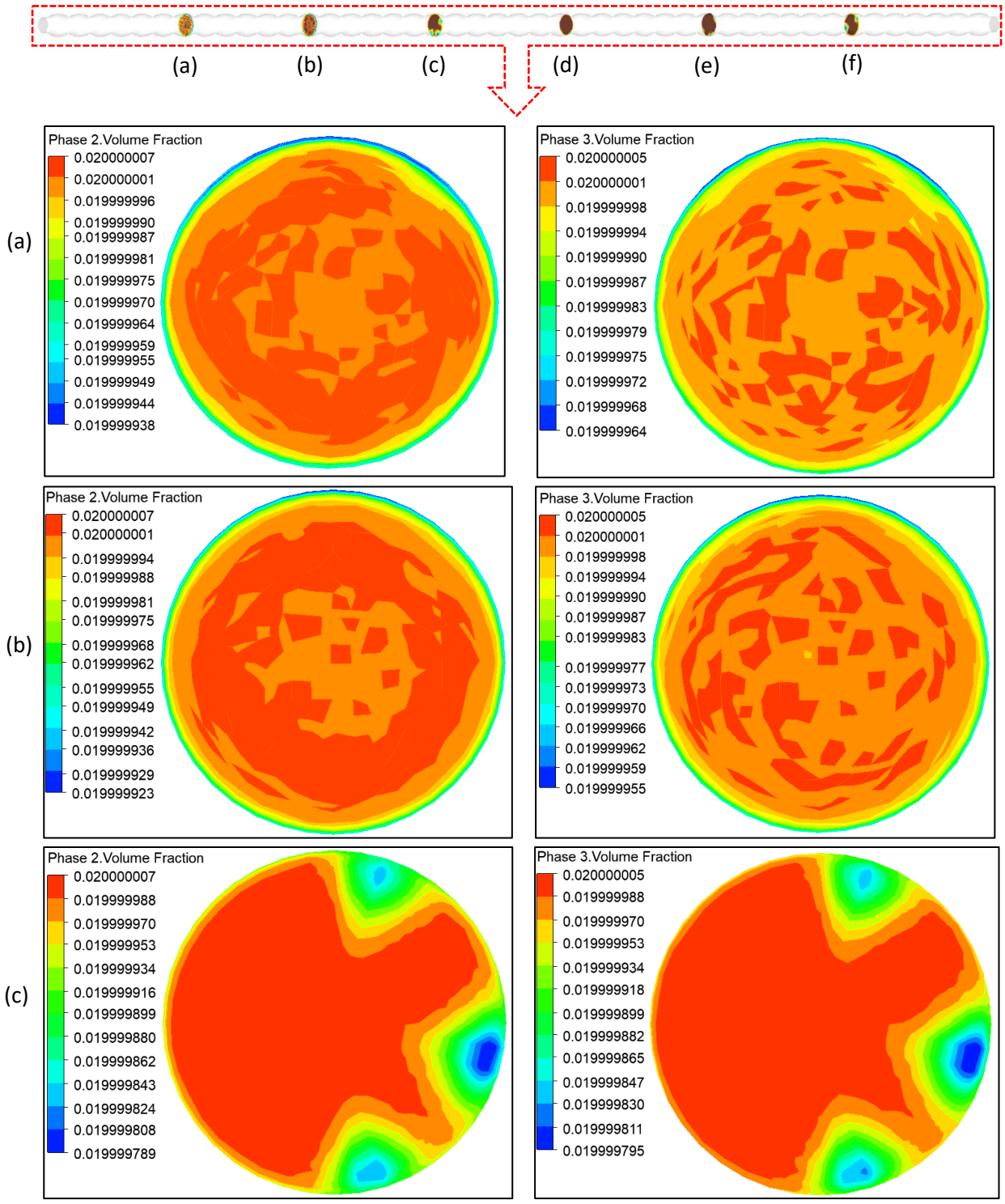

Figure 9: Contours of nanoparticles volume fraction distribution at $\varphi = 2\%$ and $Re = 31{,}331$ along various cross-sections (a - f)

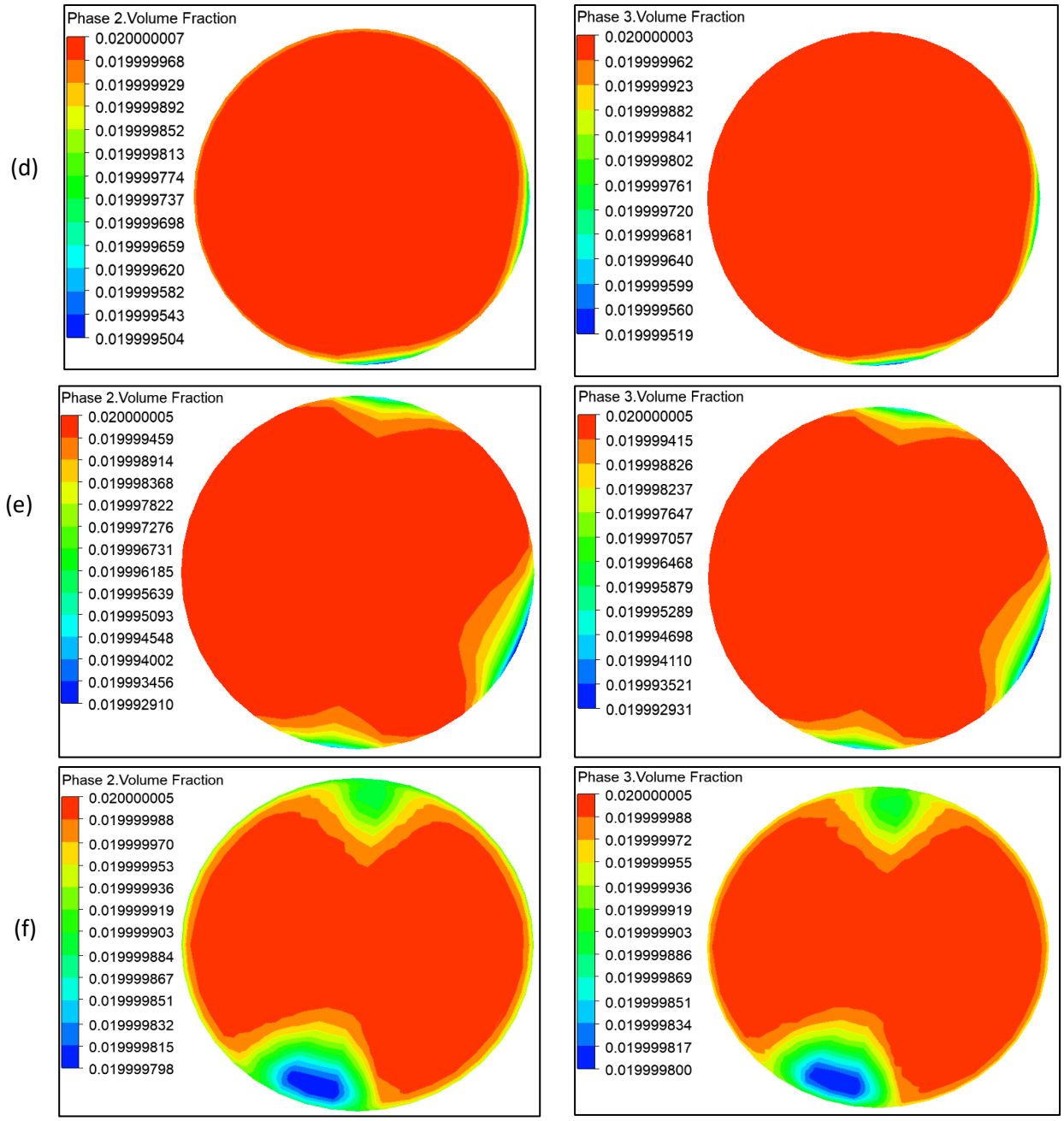

Figure 9: Continued

6. New Correlations

The Nusselt number plays a vital role in the prediction of the heat transfer for hybrid Nano-fluids. Recently, many articles were published on some correlations to estimate the friction factor and Nusselt number for hybrid Nano-fluids [51,61-65]. Such correlations are only workable for the studied Nano-fluids or the base fluid and can be implemented for particular types of Nano-fluids, ranges of Reynolds numbers, and volume concentrations.

The general equations are given by:

$$Nu = a\, Re^{w} Pr^{x} \varphi^{y} AR^{z} \tag{27}$$

$$f = a\, Re^{w} \varphi^{y} AR^{z} \tag{28}$$

Where $a, w, x, y \text{ and } z$ are constants and depend on specific discussed cases of each author. The terms $(1 + AR)$ and $(1 + \varphi)$ may appear for plain tube and base fluid correlations (when φ and $AR = 0$), respectively. Also, it was found that some authors neglect the dependence of Nusselt number on volume concentrations, including Huang et al. [64]. In this regard, new correlations were developed according to Eqs. (27) and (28) to validate the numerical friction factor and Nusselt number for the hybrid Nano-fluid. The new suggested correlations are expressed as:

$$Nu = 0.000121\, Re^{0.869} Pr^{2.918} (1+\varphi)^{22.213} (1+AR)^{0.489} \quad (29)$$

$$f = 0.263\, Re^{-0.24} (1+\varphi)^{8.147} (1+AR)^{0.551} \quad (30)$$

The above-proposed correlations Eqs. (29)and (30) can be applied for hybrid Nano-fluids or base fluid under the turbulent flow condition with $0.5\% \leq \varphi \leq 2$ % and Reynolds number ranging from 3,916 to 31,331 for wavy and plain tubes. It was noticed that the current correlations were in good agreement with the obtained numerical findings with the maximum variation of ± 10.7% and ± 6.4%, respectively, as depicted in Figure 10 (a) and (b). Thus, the current correlations can be useful in estimating the thermal and hydrodynamics characteristics for a particular volume fractions of hybrid Nano-fluid.

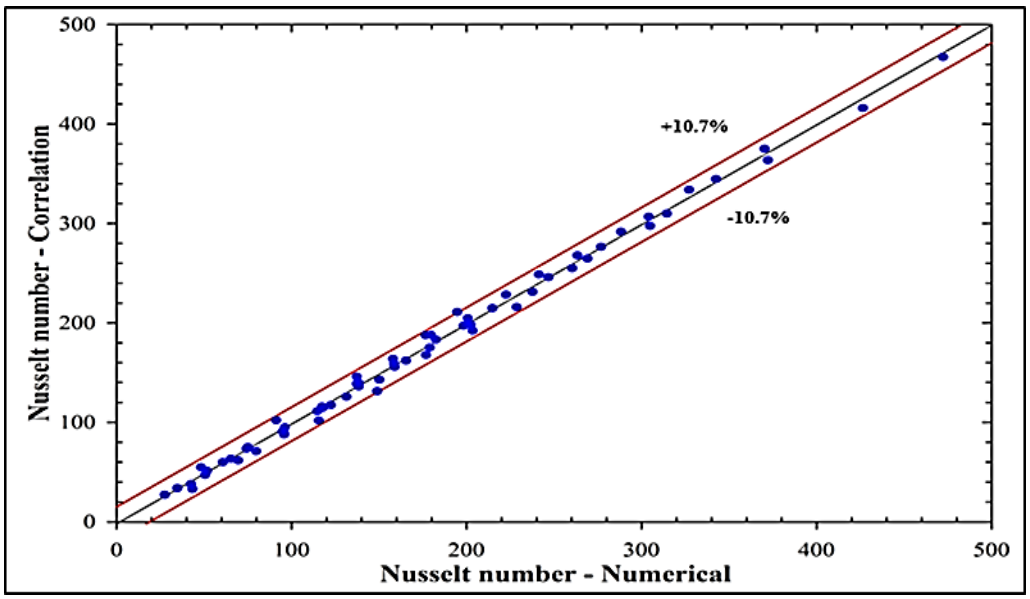

(a)

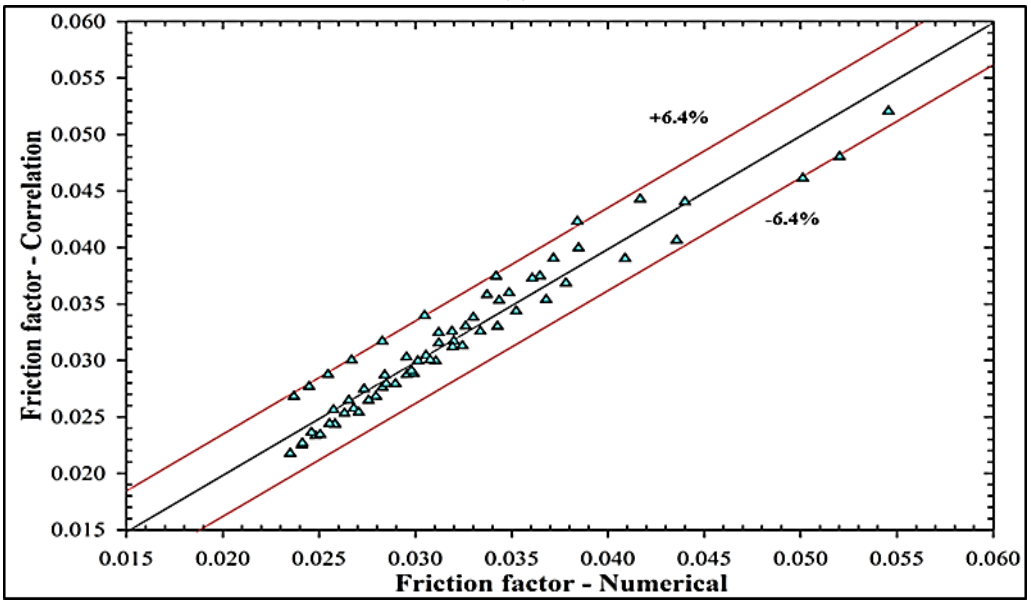

(b)

Figure 10: The numerical versus predicted (a) Average Nusselt number, and (b) friction factor based on the new correlations

7. Conclusion

This numerical research investigated the thermal and hydrodynamics behavior of the turbulent flow condition of a new hybrid Nano-fluid by employing a two-phase mixture approach. A mixture of Fe_3O_4 and MgO nanoparticles in pure water is considered with a volume concentration range of ($0.5\% \leq \boldsymbol{\varphi} \leq 2\%$) inside the uniformly heated 3D wavy and plain tubes model. The following outcomes are obtained:

- Augmenting the Reynolds number enhances the HTC and lowers the friction factor along both tubes. Also, the HTC enhancement appears to be more pronounced at $\boldsymbol{\varphi}$ = 2% in both tube types. However, the estimated average HTC of the wavy wall tube is higher compared with the conventional tube.
- It was observed that, at volume concentrations (0.5,1, and 2) %, the average enhancement in HTC is (68.7, 102.1, and 151.6) % along the wavy tube; and (59.4, 80.4, and 113.6) % along the plain tube, respectively.
- The highest attainable HPI of the hybrid Nano-fluid through a wavy wall tube is (2.41), which belongs to the 2% volume concentration at Re=31,331.
- New correlations were suggested for a specific volume fraction of the hybrid Nano-fluid.

Nomenclature

AR	Amplitude ratio $\left(\frac{2a}{D}\right)$
$\boldsymbol{a}$	Amplitude (mm)
$\boldsymbol{D}$	Diameter (mm)
Pr	Prandtl number
Nu	Nusselt number
$\boldsymbol{P}$	Pressure ($kg\ m^{-1}\ s^{-2}$)
$\boldsymbol{Re}$	Reynolds number
$\boldsymbol{T}$	Temperature (K)
$\boldsymbol{f}$	Friction factor
$\boldsymbol{g}$	Gravitational acceleration ($m\ s^{-2}$)
$\boldsymbol{t}$	Time (s)
$\boldsymbol{u}$	Velocity ($m\ s^{-1}$)

Greek letters

$\boldsymbol{\lambda}$	Wavy-length (mm)
$\boldsymbol{\mu}$	Dynamic viscosity($kg\ m^{-1}\ s^{-1}$)
$\boldsymbol{\rho}$	Density($kg\ m^{-3}$)
$\boldsymbol{\varphi}$	Volume concentration (%)

Subscripts

av.	Average
eff	Effective
$\boldsymbol{f}$	Base fluid
$\boldsymbol{np}$	Nanoparticle
$\boldsymbol{nf}$	Nano-fluid

Acknowledgment

Acknowledgments may be directed to individuals or institutions that have contributed to the research or a government agency.

Author contributions

All authors contributed equally to this work.

Funding

This research received no specific grant from any funding agency in the public, commercial, or not-for-profit sectors.

Data availability statement

The data that support the findings of this study are available on request from the corresponding author.

Conflicts of interest

The authors declare that there is no conflict of interest.

References

[1] A.A. Karamallah, H.H. Abed, Experimental Investigation of Combined Effect of Particle Size and Stability of Al2O3-H2O Nanofluid on Heat Transfer Augmentation Through Horizontal Pipe. Eng. Technol. J., 38, (2020) 561-573. https://doi.org/10.30684/etj.v38i4A.177

[2] K. F. Sultan, A. A. Karamallah, Experimental Investigation of Heat Transfer Enhancement and Flow with Ag, Tio2ethylene Glycol distilled Waternanofluid in Horizontal Tube. Eng. Technol. J., 32 (2014) 461-485. https://doi.org/:10.30684/etj.32.3B.9

[3] D.D.Vo, et al., Effectiveness of various shapes of Al_2O_3 nanoparticles on the MHD convective heat transportation in porous medium, J. Therm. Anal. Calorim., 139 (2020) 1345-1353. https://doi.org/10.1007/s10973-019-08501-4

[4] S.A. Shehzad, et al., Convective MHD flow of hybrid-nanofluid within an elliptic porous enclosure. Phys. Lett. A, 384 (2020) 126727. https://doi.org/10.1016/j.physleta.2020.126727

[5] B. Bakthavatchalam, et al., Comprehensive study on nanofluid and ionanofluid for heat transfer enhancement: A review on current and future perspective. J. Mol. Liq., 305 (2020) 112787. https://doi.org/10.1016/j.molliq.2020.112787

[6] A. A. Karamallah, N. S. Mahmoud, Experimental Investigation of Heat Transfer Enhancement with Nanofluid and Twisted Tape Inserts in a Circular Tube. Eng. Technol. J., 34 (2016) 664-684. https://doi.org/10.30684/etj.34.3A.19

[7] M. Mahmoodi, Sh. Kandelousi, Effects of thermophoresis and Brownian motion on nanofluid heat transfer and entropy generation. J. Mol. Liq., 211 (2015) 15-24. https://doi.org/10.1016/j.molliq.2015.06.057

[8] L. T. Benos, I.E. Sarris, The interfacial nanolayer role on magnetohydrodynamic natural convection of an Al2O3-water nanofluid. Heat Transfer Eng., 42 (2021) 89-105. https://doi.org/10.1080/01457632.2019.1692487

[9] Shehzad, S., et al., Heat transfer management of hybrid nanofluid including radiation and magnetic source terms within a porous domain. Appl. Nanosci. , 10 (2020) 5351-5359. https://doi.org/10.1007/s13204-020-01432-9

[10] G. Liang, I. Mudawar, Review of single-phase and two-phase nanofluid heat transfer in macro-channels and micro-channels. Int. J. Heat Mass Transfer, 136 (2019) 324-354. https://doi.org/10.1016/j.ijheatmasstransfer.2019.02.08

[11] S.E. Maiga, et al., Heat transfer enhancement by using nanofluids in forced convection flows. Int. J. Heat Fluid Flo, 26 (2005) 530-546. https://doi.org/10.1016/j.ijheatfluidflow.2005.02.004

[12] S.E. Maïga, et al., Heat transfer enhancement in turbulent tube flow using Al_2O_3 nanoparticle suspension, Int. J. Numer. Methods for Heat & Fluid Flow, 16 (2006) 275-292. https://doi.org/10.1108/09615530610649717

[13] A. Behzadmehr, M. Saffar-Avval, N. Galanis, Prediction of turbulent forced convection of a nanofluid in a tube with uniform heat flux using a two phase approach, Int. J. Heat Fluid Flow, 28 (2007) 211-219. https://doi.org/10.1016/j.ijheatfluidflow.2006.04.006

[14] B. Mahanthesh, et al., Significance of Joule heating and viscous heating on heat transport of MoS2–Ag hybrid nanofluid past an isothermal wedge. J. Therm. Anal. Calorim., 143 (2021) 1221-1229. https://doi.org/10.1007/s10973-020-09578-y

[15] S.A. Shehzad, et al., Examination of CVFEM for nanofluid free convection MHD flow through permeable medium. Appl. Nanosci., 10 (2020) 3269-3277. https://doi.org/10.1007/s13204-020-01316-y

[16] M.K. Moraveji, E. Esmaeili, Comparison between single-phase and two-phases CFD modeling of laminar forced convection flow of nanofluids in a circular tube under constant heat flux. Int. Commun. Heat Mass Transfer, 39 (2012) 1297-1302. https://doi.org/10.1016/j.icheatmasstransfer.2012.07.012

[17] A. Albojamal, K. Vafai, Analysis of single phase, discrete and mixture models, in predicting nanofluid transport. Int. J. Heat Mass Transfer, 114 (2017) 225-237. https://doi.org/10.1016/j.ijheatmasstransfer.2017.06.030

[18] I. Behroyan, et al., Turbulent forced convection of Cu–water nanofluid: CFD model comparison. Int. Commun. Heat Mass Transfer, 67 (2015) 163-172. https://doi.org/10.1016/j.icheatmasstransfer.2015.07.014

[19] T. Ambreen, A. Saleem, C.W. Park, Analysis of hydro-thermal and entropy generation characteristics of nanofluid in an aluminium foam heat sink by employing Darcy-Forchheimer-Brinkman model coupled with multiphase Eulerian model. Appl. Therm. Eng., 173 (2020) 115231. https://doi.org/10.1016/j.applthermaleng.2020.115231

[20] M. Shafahi, et al., Thermal performance of flat-shaped heat pipes using nanofluids. Int. J. Heat Mass Transfer, 53 (2010) 1438-1445. https://doi.org/10.1016/j.ijheatmasstransfer.2009.12.00

[21] A. Moghadassi, E. Ghomi, and F. Parvizian, A numerical study of water based Al2O3 and Al2O3–Cu hybrid nanofluid effect on forced convective heat transfer. Int. J. Therm. Sci.,92 (2015) 50-57. https://doi.org/10.1016/j.ijheatmasstransfer.2009.12.00

[22] M. Bahiraei, A numerical study of heat transfer characteristics of CuO–water nanofluid by Euler–Lagrange approach. J. Therm. Anal. Calorim., 123 (2016) 1591-1599. https://doi.org/10.1007/s10973-015-5031-0

[23] M.H. Fard, M.N. Esfahany, M. Talaie, Numerical study of convective heat transfer of nanofluids in a circular tube two-phase model versus single-phase model. Int. Commun. Heat Mass Transfer, 37 (2010) 91-97. https://doi.org/10.1016/j.icheatmasstransfer.2009.08.003

[24] I. Behroyan, et al., A comprehensive comparison of various CFD models for convective heat transfer of Al2O3 nanofluid inside a heated tube. Int. Commun. Heat Mass Transfer, 70 (2016) 27-37. https://doi.org/10.1016/j.icheatmasstransfer.2015.11.001

[25] M. S. Mojarrad, A. Keshavarz, A. Shokouhi, Nanofluids thermal behavior analysis using a new dispersion model along with single-phase. Heat Mass Transfer, 49 (2013) 1333-1343. https://doi.org/10.1007/s00231-013-1182-3

[26] E. E. Bajestan, et al., Experimental and numerical investigation of nanofluids heat transfer characteristics for application in solar heat exchangers. Int. J. Heat Mass Transfer, 92 (2016) 1041-1052. https://doi.org/10.1016/j.ijheatmasstransfer.2015.08.107

[27] M. N. Labib, et al., Numerical investigation on effect of base fluids and hybrid nanofluid in forced convective heat transfer. Int. J. Therm. Sci., 71 (2013) 163-171. https://doi.org/10.1016/j.ijthermalsci.2013.04.003

[28] N. Kumar, B. Puranik, Numerical study of convective heat transfer with nanofluids in turbulent flow using a Lagrangian-Eulerian approach. Appl. Therm. Eng., 111 (2017) 1674-1681. https://doi.org/10.1016/j.applthermaleng.2016.08.038

[29] M. Hejazian, M.K. Moraveji, A. Beheshti, Comparative study of Euler and mixture models for turbulent flow of Al2O3 nanofluid inside a horizontal tube. Int. Commun. Heat Mass Transfer, 52 (2014) 152-158. https://doi.org/10.1016/j.icheatmasstransfer.2014.01.022

[30] S. Göktepe, K. Atalık, H. Ertürk, Comparison of single and two-phase models for nanofluid convection at the entrance of a uniformly heated tube. Int. J. Therm. Sci., 80 (2014) 83-92. https://doi.org/10.1016/j.ijthermalsci.2014.01.014

[31] R. Davarnejad, M. Jamshidzadeh, CFD modeling of heat transfer performance of MgO-water nanofluid under turbulent flow. Eng. Sci. Technol. Int. J., 18 (2015) 536-542. https://doi.org/10.1016/j.jestch.2015.03.011

[32] R. Lotfi, Y. Saboohi, A. M. Rashidi, Numerical study of forced convective heat transfer of nanofluids: comparison of different approaches. Int. Commun. Heat Mass Transfer, 37 (2010) 74-78. https://doi.org/10.1016/j.icheatmasstransfer.2009.07.013.

[33] M. Akbari, N. Galanis, A. Behzadmehr, Comparative analysis of single and two-phase models for CFD studies of nanofluid heat transfer. Int. J. Therm. Sci., 50 (2011) 1343-1354. https://doi.org/10.1016/j.ijthermalsci.2011.03.008

[34] M. Akbari, N. Galanis, A. Behzadmehr, Comparative assessment of single and two-phase models for numerical studies of nanofluid turbulent forced convection. Int. J. Heat Fluid Flow, 37 (2012) 136-146. https://doi.org/10.1016/j.ijheatfluidflow.2012.05.005

[35] L. S. Sundar, M. K. Singh, A. C. Sousa, Enhanced heat transfer and friction factor of MWCNT–Fe3O4/water hybrid nanofluids. Int. Commun. Heat Mass Transfer, 52 (2014) 73-83. https://doi.org/10.1016/j.icheatmasstransfer.2014.01.012

[36] L. Zhixiong, et al., Numerical assessment on the hydrothermal behavior and irreversibility of MgO-Ag/water hybrid nanofluid flow through a sinusoidal hairpin heat-exchanger. Int. Commun. Heat Mass Transfer, 115 (2020) 104628. https://doi.org/10.1016/j.icheatmasstransfer.2020.104628

[37] M. Rashidi, et al., Comparative numerical study of single and two-phase models of nanofluid heat transfer in wavy channel. Appl. Math. Mech., 35 (2014) 831-848. https://doi.org/10.1007/s10483-014-1839-9

[38] A. Alshare, W. Al-Kouz, W. Khan, Cu-Al2O3 Water Hybrid Nanofluid Transport in a Periodic Structure. Processes, 8 (2020) 285. https://doi.org/10.3390/pr8030285

[39] O. Mahian, et al., Recent advances in modeling and simulation of nanofluid flows-Part I: Fundamentals and theory. Physics reports, 790 (2019) 1-48. https://doi.org/10.1016/j.physrep.2018.11.004

[40] O. Mahian, et al., Recent advances in modeling and simulation of nanofluid flows-part II: applications. vol. 791. Phys Rep, 791 (2019) 1-59. https://doi.org/10.1016/j.physrep.2018.11.003

[41] A.S. Habeeb, A.A. Karamallah, S. Aljabair, Review of Computational Multi-Phase Approaches of Nano-fluids Filled Systems. Therm. Sci. Eng. Prog. , 28 (2021) 101175. https://doi.org/10.1016/j.tsep.2021.101175

[42] L. Zhixiong., et al., Numerical assessment on the hydrothermal behavior and irreversibility of MgO-Ag/water hybrid nanofluid flow through a sinusoidal hairpin heat-exchanger. Int. Commun. Heat Mass Transfer, 115 (2020) 104628. https://doi.org/10.1016/j.icheatmasstransfer.2020.104628

[43] L. S. Sundar, M. T. Naik, K. V. Sharma,M. K. Singh, T. Ch. Siva, Experimental investigation of forced convection heat transfer and friction factor in a tube with Fe 3 O 4 magnetic nanofluid. Exp. Therm Fluid Sci., 37 (2012) 65-71. https://doi.org/10.1016/j.expthermflusci.2011.10.004

[44] A.C. Yunus, Heat transfer: a practical approach. MacGraw Hill, New York. 2003.

[45] M. Abbasi, Z. Baniamerian, Analytical simulation of flow and heat transfer of two-phase nanofluid (stratified flow regime). Int. J. Chem. Eng., 2014. https://doi.org/10.1155/2014/474865

[46] M. Hatami, D.D. Ganji, M. Gorji-Bandpy, CFD simulation and optimization of ICEs exhaust heat recovery using different coolants and fin dimensions in heat exchanger. Neural Comput. Appl., 25 (2014) 2079-2090. https://doi.org/10.1007/s00521-014-1695-9

[47] H. Maddah, et al., Factorial experimental design for the thermal performance of a double pipe heat exchanger using Al2O3-TiO2 hybrid nanofluid. Int. Commun. Heat Mass Transfer, 97 (2018) 92-102. https://doi.org/10.1016/j.icheatmasstransfer.2018.07.002

[48] R. H. Notter, C. A. Sleicher, A solution to the turbulent Graetz problem—III Fully developed and entry region heat transfer rates. Chem. Eng. Sci., 27 (1972) 2073-2093. https://doi.org/10.1016/0009-2509(72)87065-9

[49] F. Incropera, D. DeWitt, Diffusion mass transfer. Fundamentals of heat and mass transfer. 4th ed. New York: John Wiley & Sons, (1996) 784-5.

[50] Bergman, T.L., et al., Fundamentals of heat and mass transfer. 2011: John Wiley & Sons.

[51] X. Fang, Y. Xu, Z. Zhou, New correlations of single-phase friction factor for turbulent pipe flow and evaluation of existing single-phase friction factor correlations. Nucl. Eng. Des., 241 (2011) 897-902. https://doi.org/10.1016/j.nucengdes.2010.12.019

[52] B. S. Petukhov, Heat transfer and friction in turbulent pipe flow with variable physical properties, in Advances in heat transfer. 6 (1970) 503-564. https://doi.org/10.1016/S0065-2717(08)70153-9

[53] D. D. Vo, et al., Numerical investigation of γ-AlOOH nano-fluid convection performance in a wavy channel considering various shapes of nanoadditives. Powder Technol., 345 (2019) 649-657. https://doi.org/10.1016/j.powtec.2019.01.057

[54] Minea, A.Adriana, Hybrid nanofluids based on Al2O3, TiO2 and SiO2: Numerical evaluation of different approaches. Int. J. Heat Mass Transfer, 104 (2017) 852-860. https://doi.org/10.1016/j.ijheatmasstransfer.2016.09.012

[55] M. M. Heyhat, et al., Experimental investigation of turbulent flow and convective heat transfer characteristics of alumina water nanofluids in fully developed flow regime. Int. Commun. Heat Mass Transfer, 39 (2012) 1272-1278. https://doi.org/10.1016/j.icheatmasstransfer.2012.06.024

[56] W. Peng, et al., Comparison of multidimensional simulation models for nanofluids flow characteristics. Numer. Heat Transfer, Part B, 63 (2013) 62-83. https://doi.org/10.1080/10407790.2012.724993

[57] A. Albojamal, et al., Analysis of nanofluid transport through a wavy channel. Numer. Heat Transfer, Part A, 72 (2017) 869-890. https://doi.org/10.1080/10407782.2017.1412679

[58] A. S. Habeeb, S. Aljabair, A.A. Karamallah, Experimental and Numerical Assessment on Hydrothermal Behaviour of MgO-Fe3O4/H2O Hybrid Nano-fluid. Int. J. Thermofluids, 16 (2022) 100231. https://doi.org/10.1016/j.ijft.2022.100231

[59] M. Mahdavi, M. Sharifpur, J.P. Meyer, CFD modelling of heat transfer and pressure drops for nanofluids through vertical tubes in laminar flow by Lagrangian and Eulerian approaches. Int. J. Heat Mass Transfer, 88 (2015) 803-813. https://doi.org/10.1016/j.ijheatmasstransfer.2015.04.112

[60] N. H. Mahmel, Y. Shekari, A. Tayebi, Three-dimensional analysis of forced convection of Newtonian and non-Newtonian nanofluids through a horizontal pipe using single-and two-phase models. Int. Commun. Heat Mass Transfer, 121 (2021) 105119. https://doi.org/10.1016/j.icheatmasstransfer.2021.105119

[61] D. K. Devendiran, V.A. Amirtham, A review on preparation, characterization, properties and applications of nanofluids. Renewable Sustainable Energy Rev., 60 (2016) 21-40. https://doi.org/10.1016/j.rser.2016.01.055

[62] G. Huminic, A. Huminic, Application of nanofluids in heat exchangers: A review. Renewable Sustainable Energy Rev., 16 (2012) 5625-5638. https://doi.org/10.1016/j.rser.2012.05.023

[63] R. Nimmagadda, K. Venkatasubbaiah, Conjugate heat transfer analysis of micro-channel using novel hybrid nanofluids (Al2O3+ Ag/Water). European Journal of Mechanics-B/Fluids, 52 (2015) 19-27. https://doi.org/10.1016/j.euromechflu.2015.01.007

[64] D. Huang, Z. Wu, B. Sunden, Effects of hybrid nanofluid mixture in plate heat exchangers. Exp. Therm Fluid Sci., 72 (2016) 190-196. https://doi.org/10.1016/j.expthermflusci.2015.11.009.

[65] G. Huminic, A. Huminic, Heat transfer and flow characteristics of conventional fluids and nanofluids in curved tubes: a review. Renewable Sustainable Energy Rev., 58 (2016) 1327-1347. https://doi.org/10.1016/j.rser.2015.12.230